DISPERSION, TUNABILITY AND APPLICATIONS OF DEFECT MODES IN PHOTONIC BAND-GAP STRUCTURES

R.D. PECHSTEDT, P.ST.J. RUSSELL and T.A. BIRKS
Optoelectronics Research Centre, University of Southampton, Southampton SO17 1BJ, U.K.

1. Introduction

Electronic surface states, whose energies lie within the semiconductor band-gap, are normally regarded as a nuisance to be avoided in semiconductor lasers. This is particularly true of micro-pillar laser arrays where the surface-area-to-volume ratio is large. Similarly, intra-*photonic*-band-gap interface or surface states will reduce the effectiveness of a photonic bandgap material by introducing intra-band-gap states into which unwanted spontaneous emission and lasing can occur [1,2]. These *photonic defect states* are not, however, always undesirable. Examples include: i) the DFB laser mode supported by a structural defect at the centre of a uniform Bragg mirror - the resonant frequency of this mode lies within the photonic bandgap of the Bragg mirror [3]; ii) the surface-guided Bloch modes (SGBM) confined at the surface of multilayer stacks [4]; and iii) Bragg waveguide modes (BWGM) in which total internal reflection is replaced by Bragg reflection between two multilayer stacks [4]. A general feature of defect modes is a phase velocity that is highly sensitive both to optical frequency and to the "strength" of the local aperiodicity that defines the defect. Small compositional and structural changes can radically alter the position of the mode within the stop-band, providing an effective tuning mechanism. Owing to these and other unique properties, defect modes may provide the basis for the development of a versatile new family of optoelectronic devices.

In this paper we discuss some properties of SGBM's within the context of photonic bandgaps and show how they can be used to realize a tunable narrow-band fibre tap and a mode-selective fibre coupler.

2. The Band Structure

For completeness and clarity we now outline the results of the transfer matrix analysis, given in full in [4,5]. Let us consider a dielectric multilayer stack consisting of alternating planar layers with constant refractive indices n_1, n_2 and widths h_1, h_2, respectively. The stack period Λ equals $h_1 + h_2$ and a Cartesian system of co-ordinates is used with y (z) normal (parallel) to the layers; there is no field variation with x. Due

to the planar geometry the solutions for the electromagnetic field within the stack separate into TE and TM polarization states with $H_x = E_y = E_z = 0$ and $E_x = H_y = H_z = 0$, respectively. In each case, all field components can be expressed in terms of the remaining x component, denoted by F. The normal modes of a periodic medium are Bloch waves in the same sense as planar waves are the normal modes of a homogeneous medium. Due to the translational symmetry of the medium, Bloch waves obey the Floquet-Bloch theorem and the following relationship holds:

$$F_{\pm}(y+\Lambda) = F_{\pm}(y)\exp(\pm i k_y \Lambda) , \tag{1}$$

where k_y is the Bloch wavevector given by

$$\cos(k_y\Lambda) = \cos(p_1 h_1)\cos(p_2 h_2) - \frac{1}{2}(r+1/r)\sin(p_1 h_1)\sin(p_2 h_2) , \tag{2}$$

where $r = p_1\xi_1/p_2\xi_2$ and $p_j = (k^2 n_j^2 - \beta^2)^{1/2}$ is the wavevector component normal to the interface in the j-th layer. Here k denotes the vacuum wavevector at optical frequency $\omega/2\pi$, β is the propagation constant along the z direction parallel to the layers, and ξ_j is a polarization parameter equal to 1 and $1/n_j^2$ for TE and TM polarization, respectively. The field $F(y)$ is obtained by solving Helmholtz's equation in each layer and matching the solutions in two adjacent layers via the boundary conditions. The general field in the structure (for given ω, β, and polarization) is expressible as a superposition of the two Bloch waves in Eq.(1).

If k_y is real, the Bloch waves in Eq.(1) are progressive and may transport energy normal to the layers as well as along them. If, however, values of ω and β exist for which the magnitude of the RHS of Eq.(2) exceeds 1, k_y has an imaginary part. In this case, the Bloch waves are evanescent, growing or decaying exponentially from period to period normal to the layers, while progressing along them. If the structure is infinite in the y-direction, these waves cannot be supported and no real states exist; the ranges of ω and β where this occurs are known as *stop-bands*. The band edges between real and virtual states (i.e., travelling and evanescent Bloch waves) occur when $\cos(k_y\Lambda) = \pm 1$.

By introducing a defect into the structure, real states within the stop-band can occur. In this case the Bloch waves play the role of tunnelling fields, resulting in field localization near the defect. The most radical defect is a truncation. In a truncated structure, photonic surface waves can form when the external field is evanescent and matches to a Bloch wave decaying into the stack. This is the case of a SGBM, the properties of which will be considered in more detail in the next section. On the other hand, by changing the thickness of only one layer in a particular period or replacing it with a layer of different refractive index, a structural or compositional defect can easily be introduced into an infinite structure. This type of defect mode corresponds to a BWGM and the degree of spatial localization is entirely determined by its position within the stop-band via the imaginary part of k_y. If a defect layer is introduced into a semi-infinite stack supporting a SGBM, hybrid modes between a SGBM and a BWGM can form.

3. Surface-Guided Bloch Modes

3.1. DISPERSION

The energy (wavevector) of Bloch waves can be quantized by truncating the medium in which they exist. This results in a reduction of the spectral density of states (i.e., the number of states per unit frequency in a given volume), caused by localizing the waves between the boundaries. Here the simplest case of a semi-infinite periodic medium with a common interface to an isotropic external medium with refractive index n_{ext} will be considered, leading to a single SGBM. It propagates within the plane parallel to the layers of the stack and the associated field is localized near the interface with the external medium. The variety of possible localized states in periodic structures is much richer than in isotropic media due to the fact that complete reflection can be produced within ranges of β (the *stop-bands*) where the structure would be expected to be transparent when considering the average index only. Further examples of localized states supported by multilayer stacks are given in [5].

The dispersion relation of the SGBM may be shown to take the form [5]:

$$p_j \frac{h_j}{2} - \arctan\left(\frac{\xi_e p_e \Lambda a_j + b_j}{\xi_j p_j \Lambda a_j - (\xi_e p_e / \xi_j p_j) b_j}\right) = m\pi \ , \qquad (3)$$

where the parameters with subscripts j are those belonging to the last partial layer of the stack, $p_e = (\beta^2 - k^2 n_{ext}^2)^{1/2}$ is the amplitude decay rate into the external medium, and $\xi_e = 1\ (1/n_{ext}^2)$ for TE (TM) polarization. The constants a_j and b_j determine the field amplitude and can be expressed via the components of the transfer matrix.

SGBM's can exist for both TE and TM polarizations. This is in contrast to other electromagnetic surface excitations like surface plasmons (oscillations of surface charges located at the interface with a metal) which can only form for TM polarization; in the TE case, the electric field component normal to the interface E_y equals zero and hence no surface charges are generated. A SGBM, however, is confined to the interface by different mechanisms that apply to both polarization states: total internal reflection from the external medium and Bragg reflection from the multilayer stack.

Figure 1 shows the effective propagation index $n_{eff} = \beta/k$ (solving Eq.(3) for β) and the band edges as a function of wavelength $\lambda = 2\pi/k$. For all numerical simulations, a stack consisting of alternating layers of $Al_{0.1}Ga_{0.9}As$ ($n_1 = 3.58$ at 830nm, $h_1 = 65.6$nm) and AlAs ($n_2 = 2.99$ at 830nm, $h_2 = 75.4$nm) was assumed. The final untruncated layer is made of AlAs, followed by a topmost layer of $Al_{0.1}Ga_{0.9}As$ of thickness $h_{fl} = 7.3$nm. As can be seen from Fig.1, SGBM's exhibit a considerable dispersion with wavelength. This is due to the fact that the formation of a SGBM relies on Bragg reflection, the effect of which is determined by the mutual phase shifts between the waves partially backreflected from each layer of the stack. In other words, the phase velocity is highly sensitive to the optical frequency, which is a general feature of defect modes.

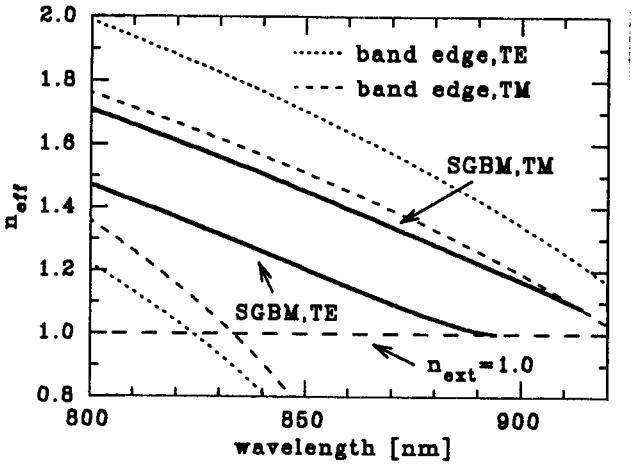

Figure 1. Stop-band edges and dispersion of SGBM's.

3.2. LOCATION WITHIN STOP-BAND

The phase velocity of defect modes is also strongly dependent on structural changes of the aperiodicity which defines the defect; an example is provided by changing the thickness of the topmost layer h_{f1} (or h_{f2}, if the topmost truncated layer consists of AlAs). The high sensitivity of SGBM's to h_{fj}, $j = 1,2$, is a result of the condition that the round-trip phase between two evanescent reflections at the interface must be an integral multiple of 2π in order to form a guided mode (this condition is equivalent to

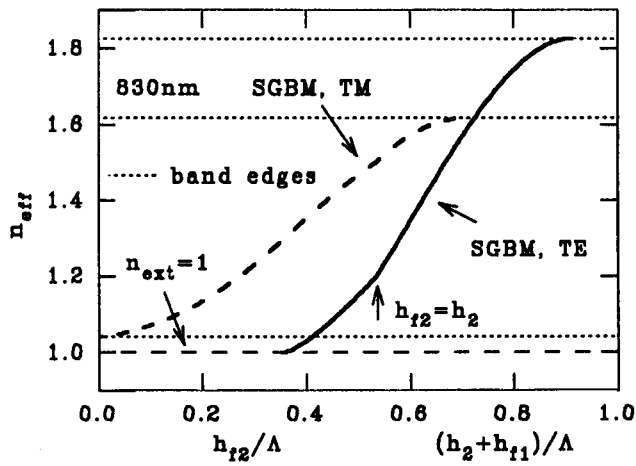

Figure 2. Effective propagation index of SGBM's versus thickness of the topmost layer.

the dispersion relation). By choosing the appropriate thickness of this layer, it is possible to place the SGBM anywhere within the stop-band, provided that n_{eff} remains larger than n_{ext} to ensure an evanescent behaviour within the external medium. This can be seen in Fig.2, where n_{eff} is plotted as a function of h_{fj}, starting with medium 2 up to h_2, followed by medium 1 up to h_1. The kink apparent in the graph for TE-polarization occurs at the position where the completed layer of medium 2 finishes (i.e., $h_{f2} = h_2$) and the next layer of medium 1 begins. Because $n_1 > n_2$, the change in round-trip phase per unit layer thickness is larger in medium 1, resulting in a steeper graph. Due to the considerable width of the stop-bands obtainable with these structures, a substantial range of quasi-single mode operation exists. For a certain range of thickness, this effect also can be used to completely suppress one or both states of polarization.

3.3. TUNING

In addition to a high sensitivity to structural changes, defect modes are also highly sensitive to compositional changes. For example, by changing the refractive index of the external medium, it is possible to tune n_{eff} as the associated field tail extends into the external medium and hence senses the refractive index n_{ext}. In Fig.3 the effective index is plotted as a function of the external index for both TE and TM-polarized SGBM's.

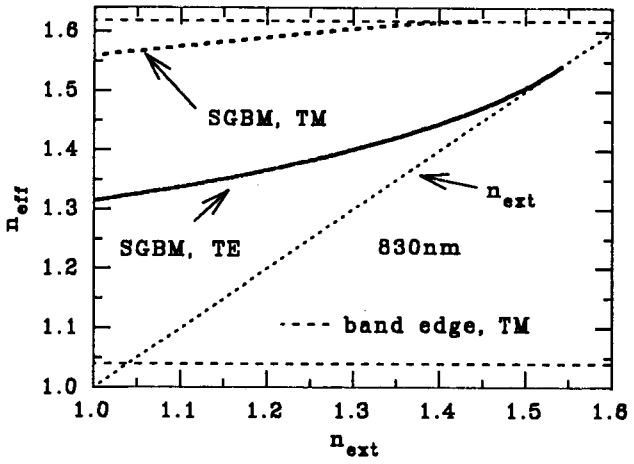

Figure 3. Effective propagation index of SGBM's versus refractive index of external medium.

The rate of change of n_{eff} with n_{ext} increases with increasing n_{ext} in the TE case. The reason is that for larger n_{eff} the difference $(n_{eff} - n_{ext})$ becomes small, so the evanescent field extends more into the external medium according to $L_{decay} \propto 1/(n_{eff}^2 - n_{ext}^2)^{1/2}$. In the TM case the increase in n_{eff} is restricted by the presence of the band edge, resulting in a reduced tunability.

4. Applications

4.1. TUNABLE NARROW-BAND FIBRE TAP

The considerable dispersion suggests that SGBM's would be useful in designing a narrow-bandwidth filter, in which a multilayer stack is brought in close contact with a side-polished section of single-mode fibre, separated from it by a layer of material (e.g., oil) with an alterable refractive index n_{oil} and a thickness h_{oil} (see Fig.4). A remaining cladding thickness of 1 μm is assumed to separate the fibre core from the oil layer. In practice, n_{oil} can be varied thermally.

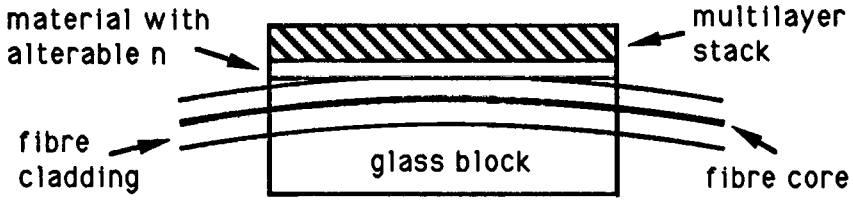

Figure 4. Generic fibre tap geometry.

Power exchange from the fibre mode to the SGBM supported by the stack occurs only if the modes are phase-matched. Due to the large difference in dispersion, the range of considerable coupling is restricted to a narrow band of wavelengths. In Fig.5 the maximum coupled power P_{max} (normalized to the input power P_o carried by the fibre mode) is shown as a function of the wavelength. In order to calculate P_{max}, the normal modes of the coupler were obtained first, modelling the fibre as a planar waveguide supporting a single mode with an appropriate effective index. Using the relationship between the normal-mode approach and coupled-mode theory [6], the coupled power follows in a straightforward manner.

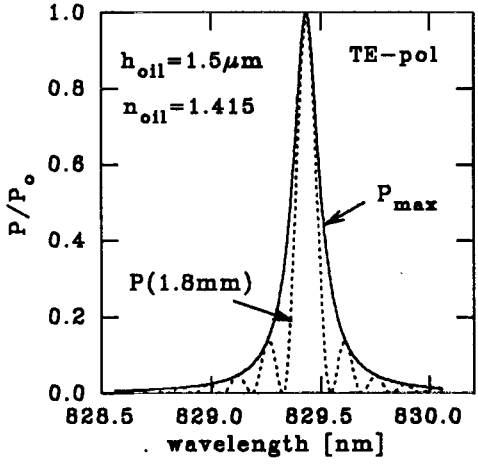

Figure 5. Maximum coupled power and power coupled at propagation length L = 1.8mm.

The maximum coupled power corresponds to the envelope of the graph obtained when calculating the power coupled to the SGBM at a fixed position $z = L$ along the fibre. An example is given by the dashed line for a coupling length equal to 1.8mm (which is the propagation distance needed to completely couple the power P_0 to the SGBM at the phase-matching point). A larger spacing h_{oil} between the fibre and stack leads to weaker coupling, resulting in a narrower bandwidth and a longer coupling length. However, the product of both remains fixed and can be used as a figure of merit to characterize the device performance; in the example considered it equals 0.3 nm mm. Due to the high sensitivity of the SGBM to the index of the intervening layer n_{oil}, good tunability is predicted. This is demonstrated in Fig.6, where the change in centre wavelength is shown as a function of n_{oil}.

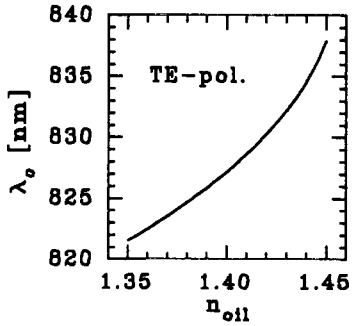

Figure 6. Centre wavelength of fibre tap versus refractive index of the oil layer.

4.2. MODE-SELECTIVE FIBRE COUPLER

Another application of SGBM's is in mode-selective coupling, where the aim is to selectively couple different spatial modes out of a multimode fibre. The device geometry is the same as in the previous section, with the single-mode fibre replaced

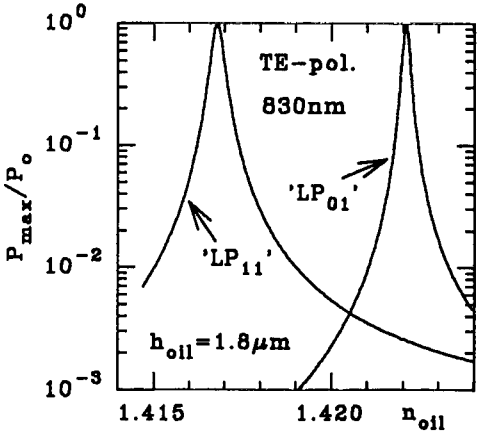

Figure 7. Maximum power coupled from each fibre mode versus refractive index of the oil layer.

by a multimode fibre. Coupling to different fibre modes is accomplished by phase matching them to the SGBM by tuning n_{oil}. Earlier experimental attempts to realize a mode-selective coupler employing surface plasmons supported by a thin metal film gave unacceptably high cross-talk from the non-phase-matched higher-order mode when phase-matched to the fundamental mode [7]. The reason is a deeper penetration of the modal field into the fibre cladding as the mode index increases, leading to a much stronger coupling. In addition, unavoidable ohmic losses in the metal layer cause a broadening of the resonances. The consequence was a trade-off between loss and selectivity, severely limiting the overall device performance. The replacement of the surface-plasmon by a virtually lossless SGBM with its higher sensitivity to the external medium results in lower cross-talk figures and better tunability. This can be seen from Fig.7, where the maximum power coupled from the modes of a two-moded fibre is shown as a function of n_{oil}. When tuned to the fundamental mode, the cross-talk from the non-phase-matched higher-order mode is ~ -26dB. When tuned to the higher-order mode, the cross-talk is ~ -36dB. These values compare favourably with the theoretical predictions for an optimized device based on surface plasmons [7], where the cross-talk figures are ~ -10dB (tuned to LP_{01}) and ~ -27dB (tuned to LP_{11}), respectively. As with the fibre tap, cross-talk figures can be decreased at the expense of a larger coupling length.

In conclusion, surface-guided Bloch modes on dielectric multilayer stacks can be regarded as a special type of defect modes in photonic band-gap structures. Owing to their unique properties they offer distinctive advantages in applications such as tunable narrow-band fibre taps and mode-selective fibre couplers.

5. Acknowledgements

The work was partly supported by the U.S. Department of the Air Force through the European Office of Aerospace Research and Development, London. The Opto-electronics Research Centre is an Interdisciplinary Research Centre of the U.K. Engineering and Physical Sciences Research Council.

6. References

1. Meade, R.D., Brommer, K.D., Rappe, A.M., and Joannopoulos, J.D. (1991) Electromagnetic Bloch waves at the surface of a photonic crystal, *Phys. Rev. A* **44**, 10961–10964.
2. Smith, D.R., Dalichaouch, R., Kroll, N., Schultz, S., McCall, S.L., and Platzman, P.M. (1993) Photonic band structure and defects in one and two dimensions, *J. Opt. Soc. Am. B* **10**, 314–321.
3. Stanley, R.P., Houdré, R., Oesterle, U., Ilegems, M., and Weisbuch, C. (1993) Impurity modes in one-dimensional systems: The transition from photonic band gaps to microcavities, *Phys. Rev. A* **48**, 2246–2249.
4. Yeh, P., Yariv, A., and Hong, Ch-S. (1977) Electromagnetic propagation in periodic stratified media. I. General theory, *J. Opt. Soc. Am.* **67**, 423–438.
5. Russell, P.St.J., Birks, T.A., and Lloyd-Lucas, F.D. (1995) Photonic Bloch Waves And Photonic Band Gaps, in E. Burstein and C. Weisbuch (eds.), *Confined Electrons and Photons: New Physics and Applications*, Plenum Press, New York, pp.585–633.
6. Vasallo, C. (1991) *Optical Waveguide Concepts*, Elsevier, Amsterdam, pp.27–35.
7. Barcelos, S., Zervas, M.N., and Russell, P.St.J. (1995) Selective excitation of fiber modes using surface plasmons, *IEEE Photon. Technol. Lett.* **7**, No.9.